Synthesis and Structure−Activity Relationship of Aminobenzophenones. A Novel Class of p38 MAP Kinase Inhibitors with High Antiinflammatory Activity

Erik Rytter Ottosen,*[,†] Morten Dahl Sørensen,[†] Fredrik Björkling,[†] Tine Skak-Nielsen,[‡] Marianne Scheel Fjording,[‡] Helle Aaes,[§] and Lise Binderup[‡]

Departments of Medicinal Chemistry, Biochemistry, and Pharmacology, LEO Pharma, Industriparken 55, DK-2750 Ballerup, Denmark

We wish to report the synthesis and structure−activity relationship (SAR) of a series of 4-aminobenzophenones, as a novel compound class with high antiinflammatory activity. Our initial lead, {4-[(2-aminophenyl)amino]phenyl}(phenyl)methanone (**3**), was systematically optimized and resulted in compounds that potently inhibited the release of the proinflammatory cytokines IL-1β and TNF-α in human peripheral blood mononuclear cells stimulated by LPS. One of the most potent compounds, among others, was {4-[(2-aminophenyl)amino]-2-chlorophenyl}(2-methylphenyl)methanone (**45**) with IC$_{50}$ values of 14 and 6 nM for the inhibition of IL-1β and TNF-α, respectively. Furthermore, we found these types of compounds to be potent and selective p38 MAP kinase inhibitors, e.g. **45** had an IC$_{50}$ value of 10 nM. Molecular modeling was used to rationalize our SAR data and to propose a model for the interaction of compound **45** with the p38 MAP kinase. The model involved a favorable hydrogen bond between the carbonyl group of the benzophenone and the NH of Met-109, positioning ring A in the hydrophobic pocket I of the enzyme. Good antiinflammatory effects were demonstrated in two murine models of dermatitis after topical application (oxazolone and TPA model).

Introduction

It is well-established that the proinflammatory cytokines interleukin-1β (IL-1β) and tumor necrosis factor-α (TNF-α) play an important role in the pathogenesis of various inflammatory diseases such as rheumatoid arthritis (RA), inflammatory bowel disease, osteoarthritis, psoriasis, endotoxemia, and/or toxic shock syndrome.[1−9] Under normal conditions, the regulated synthesis of TNF-α and IL-1β serves as a protection of the body from infectious agents, tumors, or tissue damage. But in autoimmune diseases, high production of TNF-α and IL-1β may have deleterious effects on various tissues, e.g. severe degradation of cartilage and bone in RA. Therefore, agents that down-regulate the release of TNF-α and IL-1β from inflammatory cells and reestablish a basal level are expected to have beneficial effects in the treatment of inflammatory diseases.[10,11]

Several approaches to inhibit the production of TNF-α and IL-1β have been reported, e.g. the use of soluble TNF receptors, anti-TNF antibodies, TNF-α converting enzyme inhibitors, protein tyrosine kinase inhibitors,[1,11] and IL-1 receptor antagonists.[12,13]

An additional new target for the treatment of inflammatory disorders is the mitogen-activated protein (MAP) kinase p38.[14−18] The p38 MAP kinase (p38α) is part of the stress-activated transduction cascade responsible for cytokine production. Accordingly, p38 MAP kinase is involved in the lipopolysaccharide (LPS) stimulated release of TNF-α and IL-1β from monocytes.[18−20] Furthermore, p38 MAP kinase is known to regulate the signaling cascades coupled to the TNF-α and IL-1β receptors.[8,21] Thus, regulation of TNF-α and IL-1β via inhibition of p38 MAP kinase is considered an attractive target for antiinflammatory therapy.[14,22]

The prototypical, low-molecular-weight p38 MAP kinase inhibitor triarylimidazole **1** (SB203580) is known to reduce levels of TNF-α and IL-1β both in vitro and in vivo.[15,16,23−25] Recently, several reports and reviews covering new p38 MAP kinase inhibitors have been published.[22,26−32] For example, some of the most advanced compounds, **2** (VX-745, now discontinued due to adverse neurological effects), BIRB-796, and SCIO-469, have entered phase II clinical trial for the treatment of rheumatoid arthritis.[33,34]

Our interest in this promising therapeutic principle was initiated a few years ago by the discovery of a new structural class of antiinflammatory compounds. Our starting compound **3** (Figure 1) in this work was found, in a cell-based screen, to inhibit the release of TNF-α (IC$_{50}$ = 159 nM) and IL-1β (IC$_{50}$ = 226 nM) from human peripheral blood mononuclear cells stimulated by LPS.

We now report the structure−activity optimization of these novel compounds (see the generic formula **4** in Table 1). Furthermore, it is demonstrated that analogues of this new structural class of antiinflammatory compounds are specific inhibitors of the p38α and p38β MAP kinase isoforms. To rationalize our SAR data, a molecular modeling study was performed and we propose a possible model of the interaction between our most active compounds and the p38α MAP kinase enzyme. In our animal models, the most active compounds effectively inhibited both acute and chronic dermatological inflammation.

* To whom correspondence should be addressed. Tel: +45 44 92 38 00. Fax: +45 44 94 55 10. E-mail: erik.ottosen@leo-pharma.com.
† Department of Medicinal Chemistry.
‡ Department of Biochemistry.
§ Department of Pharmacology.
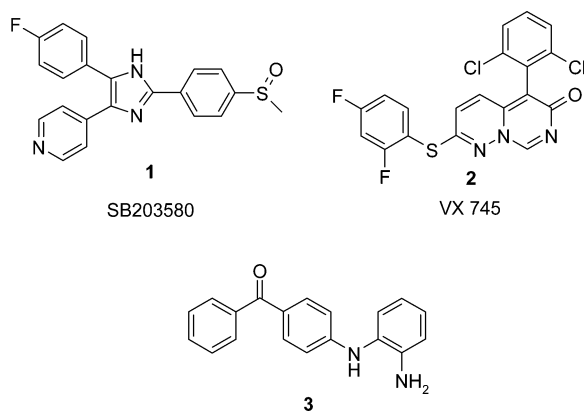
Figure 1.

Table 1. Structure Activity Data

4: X = -(CO)-; Y = H
4a: X = -(CO)-; Y = Me
4b: X = -(C=CH₂)-; Y = H
4c: X = -(CH₂)-; Y = H

compd	no.	R¹	R²	R³	IL-1β	TNF-α	anal.
			structure		IC₅₀ (nM)ᵃ	
3	4	H	H	2-NH₂	226	159	NDᵇ
35	4	2-Me	2-Cl	2-NO₂	427	382	C,H,N,Cl
40	4	2-Me	H	2-NH₂	67	47	C,H,N
41	4	3-Me	H	2-NH₂	580	467	ND
42	4	2-Br	H	2-NH₂	45	34	C,ᶜH,N
43	4	2-Ph	H	2-NH₂	483	444	C,ᶜH,N
44	4	H	2-Cl	2-NH₂	437	214	C,H,N,Cl
45	4	2-Me	2-Cl	2-NH₂	14	6	C,H,N,Cl
46	4	2-Me	3-Me	2-NH₂	343	127	ND
47	4	2-OMe	2-Cl	2-NH₂	28	20	C,H,N,Cl
48	4	2-Me	2-Me	2-NH₂	22	8	ND
49	4	2-Me	2-Cl	2-NH₂, 4-Br	30	5	C,H,N
56	4	2-Me	2-Cl	2-NHAc	21	10	C,H,N,Cl
57	4	2-Me	2-Cl	2-NHCONHEt	9	3	C,H,N,Cl
58	4	2-Me	2-Cl	2-NHCOOEt	16	6	C,H,N,Cl
60	4a	2-Me	2-Cl	2-NH₂	70	44	Cc,H,N,Clᶜ
62	4	2-Me	2-Cl	H	119	24	C,H,N,Clᶜ
63	4	2-Me	2-Cl	2-Me	26	14	C,H,N,Cl
64	4	2-Me	2-Cl	2-Me, 4-F	17	4	C,H,N,Cl
65	4	H	H	H	175	1349	ND
70	4b	2-Me	2-Cl	2-NH₂	>5000	>10000	ND
71	4c	2-Me	2-Cl	2-Me, 4-F	>10000	>10000	ND

ᵃ $n = 3$, SD (mean) = 63%. ᵇ Not determined. ᶜ Anal. not within ±0.4%.

Chemistry

We developed a general and useful synthesis of analogues of **3** with a wide variation of substituents in the three rings (Scheme 1). In short, this procedure comprised of two coupling reactions, one that gave the benzophenone and one that gave the diarylamine. We found the most efficient method in all cases was to first synthesize the benzophenone part and then the diaryl-amine part to finalize the molecule.

Substituted 4-aminobenzophenones were in general prepared by two different routes. In the first, the anion obtained by a bromo-lithium exchange reaction of the protected bromoaniline **5**[35] (commercially available, Aldrich) with *n*-butyllithium was condensed with the Weinreb amides[36] **6** and **7**, and the resulting protected benzophenones were deprotected during the aqueous workup to the aminobenzophenones **20** and **21**. Our efforts to use this strategy for the introduction of substituents in ring B were unsuccessful due to problems with the synthesis of substituted derivatives of **5**.

In our hands, the protection step[35] of readily available bromoanilines as the corresponding *N,N*-bis(trimethyl-silyl) analogues was unsatisfactory because of low yields and problems with product stability.
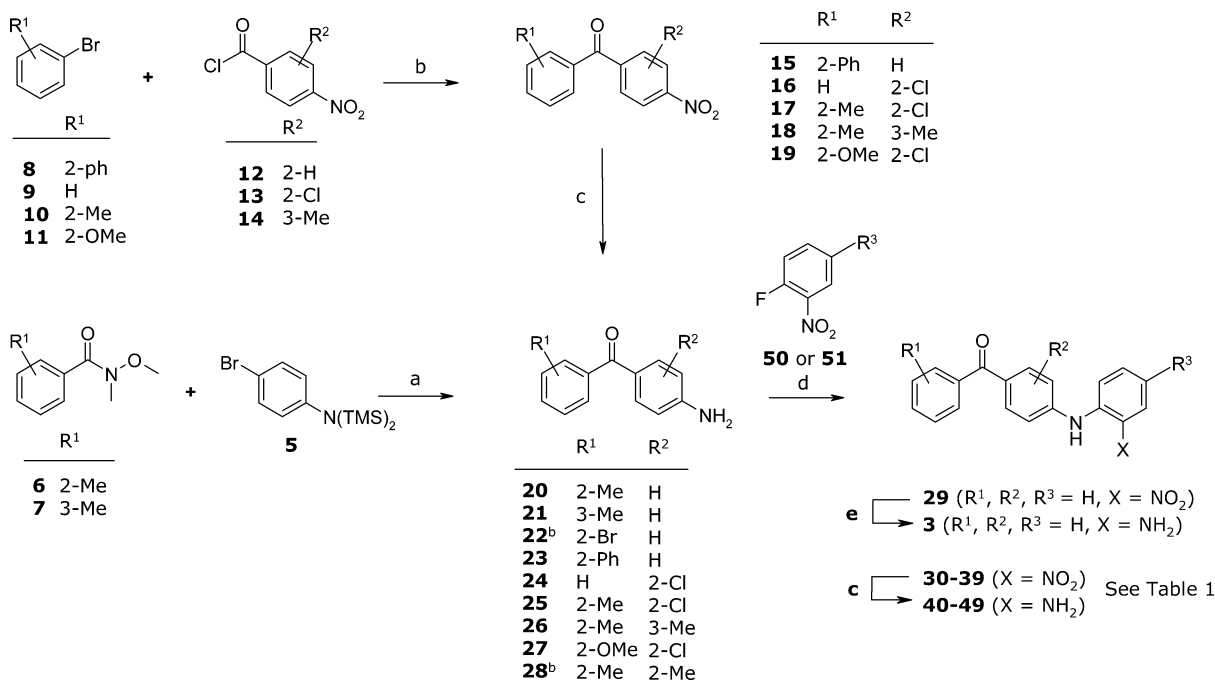
In a second approach, which allowed us to readily vary the substituents of ring A and B, a Negishi cross-coupling reaction was used as the key step.[37-39] Bromo-lithium exchange of, for example, the aryl bromide **10** gave the corresponding organolithium compound, which then was transmetalated with ZnCl₂. The resulting organozinc compound was coupled with, for example, the acid chloride **13** in the presence of tetrakis(tri-phenylphosphine)palladium(0), which gave the desired benzophenone **17**. Subsequently, reduction of the ni-trobenzophenone **17** with stannous chloride dihydrate[40] gave the aminobenzophenone **25**. The aminobenzophe-nones **23**, **24**, **26**, and **27** were synthesized using the same procedure. The yields were in the range 46–86% for the Negishi reactions and 66–98% for the reductions.

A related cross-coupling reaction was used for the preparation of the aminobenzophenones **22** and **28** (Scheme 2). The organozinc bromide obtained from **5** was readily cross-coupled with 2-bromobenzoyl chloride (**55**), as described above to give **22**. Similarly, the organozinc bromide of 2-bromotoluene (**10**) and 4-bromo-2-methylbenzoyl chloride yielded the benzophenone **53**. Interestingly, in either case no concomitant biphenyl side products were observed. This demonstrated that compared with aryl bromides, aroyl chlorides were significantly more reactive in this type of reactions. Palladium-catalyzed amination[41] of the 4-brombben-zophenone derivative **53** with benzophenone imine gave the imine **54**, which was then hydrolyzed under acidic conditions to yield **28** (Scheme 2).

Coupling[42] of 4-aminobenzophenone and the ami-nobenzophenones **20**–**28** with 2-fluornitrobenzene (**50**) and of the aminobenzophenone **25** with 5-bromo-2-fluoronitrobenzene (**51**) in the presence of potassium *tert*-butoxide gave the diarylamines **29** and **30**–**39** in moderate to good yields (Scheme 1). Reduction of the nitro group in **29** with hydrazine hydrate in the presence of a catalytic amount of palladium on carbon gave the desired compound **3**. The analogues **30**–**39** were re-duced with stannous chloride dihydrate, which gave the desired compounds **40**–**49** (Table 1). Both methods produced good to excellent yields.

The derivatives **56**–**58** were synthesized in excellent yields by standard procedures from **45** by treatment with acetic anhydride, ethyl isocyanate, or ethyl chlo-roformate. Deprotonation of the diarylamine **35** with potassium hydride, alkylation with iodomethane, and reduction of the nitro group gave the *N*-methylamino derivative **60** (Scheme 3).

Preparation of diarylamines by nucleophilc aromatic substitution of activated fluoroarenes was efficient (Scheme 1). However, we found that substitution of unactivated fluoroarenes was sluggish, even at elevated temperatures, and alternative routes for the synthesis of this type of compound were sought (Scheme 4). Palladium-catalyzed amination of bromides proved to be an efficient method.[43] Thus, coupling of aminoben-zophenone **25** with the appropriate bromide e.g. **9** using *rac*-BINAP as the ligand in the presence of either
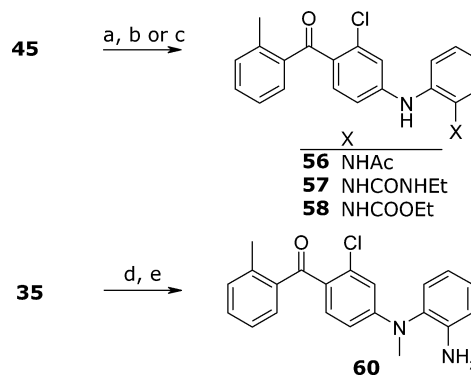
Scheme 1[a]

	R[1]	R[2]
15	2-Ph	H
16	H	2-Cl
17	2-Me	2-Cl
18	2-Me	3-Me
19	2-OMe	2-Cl

R[1]
8	2-ph
9	H
10	2-Me
11	2-OMe

R[2]
12	2-H
13	2-Cl
14	3-Me

R[1]
| **6** | 2-Me |
| **7** | 3-Me |

	R[1]	R[2]
20	2-Me	H
21	3-Me	H
22[b]	2-Br	H
23	2-Ph	H
24	H	2-Cl
25	2-Me	2-Cl
26	2-Me	3-Me
27	2-OMe	2-Cl
28[b]	2-Me	2-Me

e ⎰ **29** (R[1], R[2], R[3] = H, X = NO₂)
  ⎱ **3** (R[1], R[2], R[3] = H, X = NH₂)

c ⎰ **30-39** (X = NO₂)   See Table 1
  ⎱ **40-49** (X = NH₂)

a Reagents: (a) (i) ArBr, *n*-BuLi, Et₂O, 0 °C; (ii) Ar′CON(OMe)Me, THF, −78 to 20 °C, 24 h; (b) (i) ArBr, *n*-BuLi, THF, −78 °C, 30 min; (ii) ZnCl₂, −78 °C to rt; (iii) Ar′COCl, Pd(PPh₃)₄, rt, 18 h; (c) SnCl₂·2H₂O, EtOH, 70 °C, 2 h; (d) *t*-BuOK, DMSO, 18 h; (e) NH₂NH₂·H₂O, 10% Pd/C, rt, 24 h. *b* See Scheme 2.

Scheme 2[a]

| **53** | X = Br |
| **54** | X = HN=CPh₂ (Ph,Ph) |

56	NHAc
57	NHCONHEt
58	NHCOOEt
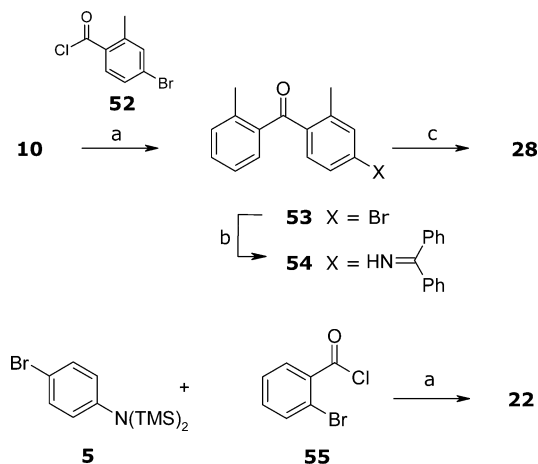
a Reagents: (a) (i) ArBr, *n*-BuLi, THF, −78 °C, 30 min; (ii) ZnCl₂, −78 °C to rt; (iii) Ar′COCl, Pd(PPh₃)₄, rt, 18 h; (b) Pd₂(dba)₃, *rac*-BINAP, *t*-BuONa, toluene, 80 °C, 48 h; (c) 2 N HCl(aq), THF, 1 h.

Scheme 3[a]

a Reagents: (a) Ac₂O, glacial acetic acid, rt, 45 min; (b) ethyl isocyanate, pyridine, rt, 4 h; (c) ethyl chloroformate, K₂CO₃, DCM, 0 °C, then 27 h at rt; (d) NaH, THF, 15 min, then MeI, reflux, 2 h; (e) SnCl₂·2H₂O, EtOH, 70 °C, 2 h.

cesium carbonate or sodium *tert*-butoxide gave **62** in good yield. The analogues **63−65** were prepared similarly.

The modified analogues **70** and **71** were obtained as described in Scheme 5. Treatment of **25** with acetonylacetone under Dean−Stark conditions gave the protected derivative **66** in quantitative yield.[44] Reaction of **66** with methyllithium led to the intermediary tertiary alcohol, which eliminated water upon treatment with acetic acid under reflux and gave the alkene **67**. Cleavage of the pyrrole was then performed with a large excess of hydroxylamine hydrochloride and triethylamine. The obtained amine **68** was coupled with 2-bromonitrobenzene to give **69**, which was reduced to the desired derivative **70**. The reduced analogue **71** was obtained directly from **64** by reduction with sodium

borohydride in trifluoroacetic acid.[45] A very low yield was obtained due to the formation of a byproduct, identified as compound **72**.

Results and Discussion

In Vitro SAR. Determination of the antiinflammatory activity of our new benzophenone compounds was made in vitro by measuring the inhibitory effect of TNF-α and IL-1β release (results summarized in Figure 2). In this primary screen, human peripheral blood mononuclear cells (PBMC's) were stimulated with LPS for release of TNF-α and IL-1β, with or without compound. Our starting compound in this structure−activity optimization, the aminobenzophenone **3**, showed an IC₅₀ of 159 and 226 nM in TNF-α and IL-1β, respectively (Table 1). Our first modification, introduction of simple substituents such as methyl, bromo, chloro, fluoro, and methoxy (data not shown) in ring A

Scheme 4[a]

	R³
62	H
63	2-Me
64	2-Me, 4-F
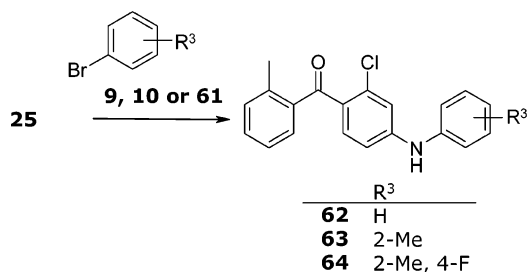
[a] Reagents: Pd₂(dba)₃, *rac*-BINAP, Cs₂CO₃, 1,4-dioxane, 100 °C, 72 h.

Scheme 5[a]

66	X = O
67	X = CH₂

71	R = H
72	R = CH₂CF₃
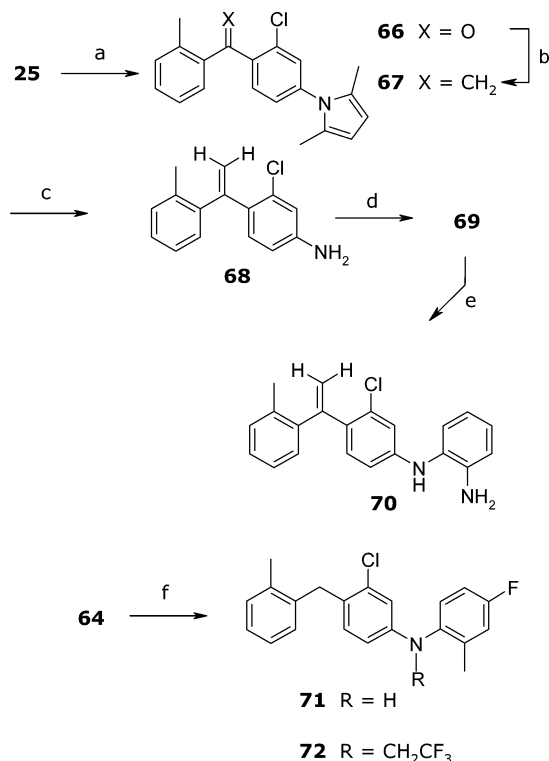
[a] Reagents: (a) Acetonylacetone, cat. TsOH·H₂O, toluene, Dean–Stark reflux 2.5 h; (b) (i) MeLi, THF, −78 °C, then warm to 10 °C (2.5 h), extraction; (ii) glacial acetic acid, reflux, 3 h; (c) HONH₂·HCl, Et₃N, EtOH/H₂O, approximately 100 °C, 24 h; (d) 2-bromonitrobenzene, Pd₂(dba)₃, *rac*-BINAP, Cs₂CO₃, 1,4-dioxane, 100 °C, 72 h; (e) SnCl₂·2H₂O, EtOH, 70 °C, 2 h; (f) CF₃COOH, NaBH₄, 0 °C, then **64** in DCM added slowly (30 min), rt, 22 h.

showed the importance of a substituent in the 2-position of ring A (e.g. **40**–**42**). Small substituents such as methyl and bromo were the most efficient, with a 3-fold increase of activity (compare **40** and **42** with **3**, and **45** with **47**). Larger substituents such as phenyl (e.g. **43**) in any position on ring A led to inactive or considerably less active compounds as compared with **3**.

Next, simple substituents were introduced in ring B. Monosubstituted analogues derived from our initial lead **3** did not result in improved activity (e.g. **44**). However, when the same set of analogues in a series related to compound **40** were prepared, increased activity was obtained (e.g. **45**, **46**, and **48**). Thus, the best compound in this series was **45**, having a 2-chloro substituent in ring B and a 2-methyl substituent in ring A. This compound was found to inhibit the TNF-α production and the IL-1β production with an IC₅₀ of 6 and 14 nM,
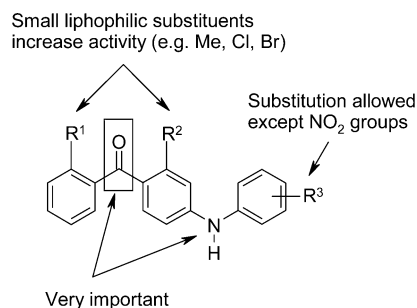

Figure 2. An overview of structure–activity relationships (SAR) of aminobenzophenones.

respectively, a 25-fold increase of activity compared to our starting compound **3**.

We speculated that these two lipophilic ortho substituents could force the benzophenone system into a more favorable conformation due to hindered rotation around the ketone bridge and initiated a modeling study (see Computational Chemistry). Introduction of substituents in the 3-position in ring B resulted in less active compounds (compare **46** and **40**). Further substitution in ring A and B did not improve the in vitro activity.

We therefore focused on ring C. Introduction of simple substituents in the 3−6-positions in ring C gave compounds with altered activities. The most interesting compounds in this series were found to be the 4-substituted analogues **49** and **64**, both with similar activity in vitro as **45**. Replacement of the primary amino group with a nitro group resulted in almost complete loss of activity (compare **45** with **35**), indicating the importance of the primary amino group for activity. However, further modifications showed that the amino group was not essential. For example the unsubstituted analogue **62** was found to be moderately active (also, compare **65** with **3**), and the 2-methyl analogues **63** and **64** were equipotent to compound **45**. Simple derivatives of **45** (amide **56**, urea **57**, and carbamate **58**) were also very active in vitro, e.g. the urea compound **57** showed an IC₅₀ of 3 nM in the TNF-α assay.

To investigate the importance of the ketone connecting rings A and B and the secondary amine connecting rings B and C, these were modified. Thus, the reduced analogue **71** and the alkene analogue **70** were both found to be inactive, indicating the importance of the ketone. Alkylation of the secondary amine was tolerated to some extent but generally gave less active compounds (e.g. **60**). Replacement of the secondary amino group in the optimized analogue **45** with, for example, oxygen or sulfur gave inactive compounds (data not shown).

Further Testing. To investigate this new structural class in more detail, some of the potent compounds were tested for their ability to inhibit a series of cytokines in whole cell assays. With the objective of getting information about the mechanism of action of our compounds, a number of known reference compounds were included. The results of compounds **45**, **49, 64,** and HEP689,[27] a p38 MAP kinase inhibitor structurally related to **2**, are shown in Table 2. Our compounds inhibited TNF-α (IC₅₀ 4−6 nM) more potently than IL-1β (IC₅₀ = 14−30 nM). Similarly, but less potently, HEP689 inhibited TNF-α (IC₅₀ = 90 nM) and IL-1β (IC₅₀ = 272 nM). The four compounds had a similar profile with respect to the inhibition of IL-6 and IL-8. Compound **49** inhibited IL-6

Table 2. Further in Vitro (IC$_{50}$, nM; n g 3) Activity of Selected Compounds

	compd			
assay	HEP689	45	49	64
IL-1β	272 ± 37	14 ± 6	30 ± 21	17 ± 15
TNF-α	90 ± 59	6 ± 1	5 ± 0	4 ± 3
IL-2	>1000	>1000[b]	>1000[b]	>1000
IL-6	125[a]	18 ± 1	17 ± 7	35 ± 28
IL-8	50[a]	6[a]	4 ± 1	79 ± 104
IL-10	71 ± 24	12 ± 8	74 ± 74	51 ± 32
IL-12	>1000	>1000	>1000[a]	>1000[a]
IFN-γ	>1000	>1000[b]	>1000	>1000

[a] $n = 1$. [b] $n = 2$.

Table 3. p38α MAP Kinase Activity Data

compd	IC$_{50}$ (nM); $n \geq 3$	compd	IC$_{50}$ (nM); $n \geq 3$
HEP689	38 ± 13	**48**	13 ± 3
VX-745	29 ± 8	**49**	39 ± 9
3	145 ± 62	**56**	63 ± 8
35	437 ± 14	**57**	21 ± 8
40	29 ± 9	**58**	42 ± 15
41	574 ± 16	**60**	101 ± 46
42	54 ± 17	**62**	7 ± 1
43	811 ± 410	**63**	12 ± 4
44	139 ± 9	**64**	4 ± 0.2
45	10 ± 3	**65**	193 ± 54
46	143 ± 26	**70**	1550 ± 190
47	5 ± 2	**71**	>100000

Table 4. Kinase Selectivity of Selected Compounds ($n = 2$)

	compd			
assay	HEP689	**45**	**49**	**64**
p38α[a]	73	88	82	88
p38β_2[a]	59	93	93	92
p38γ[a]	0	0	0	5
p38δ[a]	8	8	0	4
ERK1/2[b]	0	20	0	0
JNK1[b]	9	NT	0	0

[a] Percent inhibition at 1 μM. [b] Percent inhibition at 10 μM.

(IC$_{50}$ = 17 nM) and IL-8 (IC$_{50}$ = 4 nM) potently and was approximately 10 times more potent than HEP689 in both assays. In addition, all four compounds inhibited IL-10. None of the compounds including the literature reference compound HEP689 inhibited IL-2, IFN-γ, and IL-12 (IC$_{50}$ > 1000 nM).

Due to a cytokine inhibitory profile similar to that of the p38 MAP kinase inhibitor HEP689, our compounds and the reference compounds HEP689 and VX-745[33] were tested in a p38α MAP kinase assay (Table 3). The lead compound, **45**, was found to be a potent inhibitor of p38α kinase activity (IC$_{50}$ = 10 nM). Likewise, compound **64** (IC$_{50}$ = 4 nM) and compound **49** (IC$_{50}$ = 39 nM) inhibited p38α MAP kinase. In comparison, HEP689 and VX-745 gave IC$_{50}$ of 38 and 29 nM, respectively.

The compounds were evaluated for their in vitro kinase selectivity. Kinase assays for the four isoforms of p38 were performed using cellular transfection of the cDNA containing the respective FLAG-p38 isoform into COS-1 cells.[46,47] The kinase activity of p38α and p38β_2 was inhibited by the test compounds at 1 μM, whereas p38γ and p38δ were unaffected (Table 4). In addition, the compounds were tested in an ERK1/2 and JNK1 kinase assay using MCF-7 cells stimulated with EGF or UV light, respectively. The assays were performed using a modified cell signaling ERK1/2 kinase kit and a JNK1 kinase kit. The compounds did not inhibit the
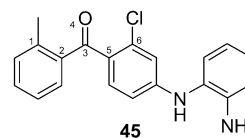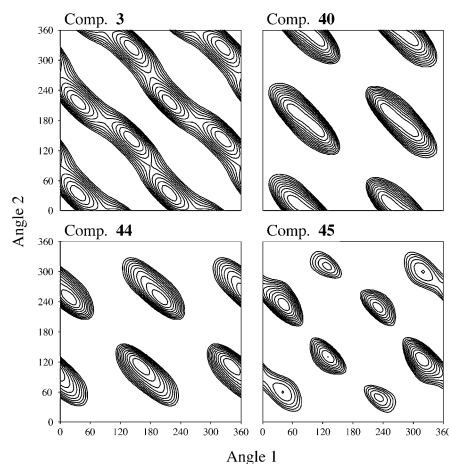
Figure 3. The carbonyl torsion angles for all conformations of **3**, **40**, **44**, and **45** within 3 kcal/mol of the global minimum. Angle 1 and 2 are defined by the atoms corresponding to 1−2−3−4 and 4−3−5−6 in **45**, respectively.

kinase activity of ERK1/2 or JNK1 when tested at 1 or 10 μM (Table 4). Furthermore, compound **49** was evaluated externally (upstate, UK) against a panel of 60 different kinases. Only three kinases (p38α, p38β, and MKK6) were inhibited by this compound at 1 μM. Thus, this new compound class was found to be highly potent and specific p38 MAP kinase inhibitors.

Computational Chemistry. We have performed an energy analysis of the two carbonyl rotations in compounds **3**, **40**, **44**, and **45**. Intuitively, one would expect that introducing ortho-substituents in ring A and B of compound **3** would restrict the rotation of these rings due to steric interactions between the substituents and the carbonyl group (Figure 3). It is immediately clear that the conformational space, as expected, becomes considerably restricted when ortho-substituents are introduced.

The higher p38α kinase activities of compounds **40** (29 nM) and **45** (10 nM) could therefore be explained by a lower entropy loss upon protein binding. This has earlier been shown for the restriction of the intramolecular rotation of a biaryl bond leading to a decreased loss of entropy upon ligand binding and thus to higher affinity.[48] Obviously, other factors may also contribute, as evidenced by compound **44**. Thus, despite the rotational restriction, compound **44** (139 nM) is equipotent to the original lead compound **3** (145 nM).

Examination of the low-energy conformations of compounds **44** and **45** reveals a difference in the preferred orientations of the carbonyl group and the chloro substituent. In compound **45** low-energy minima conformations exist where the carbonyl group is positioned either opposite to (e.g. in the global minimum conformation) or on the same side as the chloro substituent (conformations from 1.4 kcal/mol above the global minimum). In contrast, no low-energy minima conformations exist for compound **44**, where the carbonyl group and the chloro substituent are positioned on the
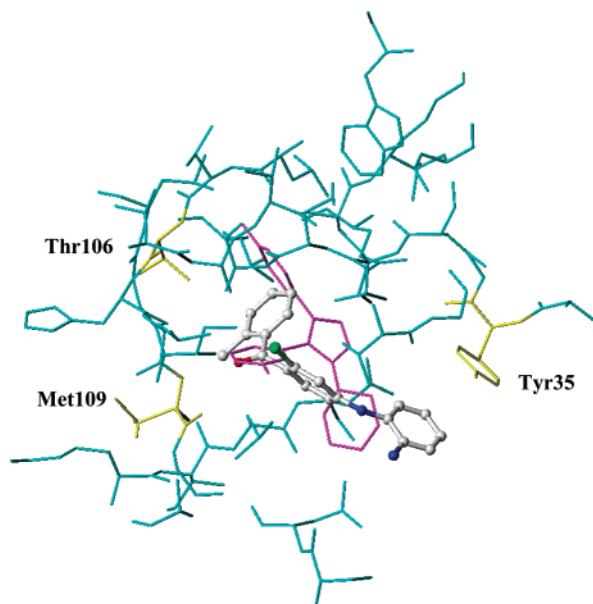
Figure 4. Model of **45** (atom colors) bound in the ATP-binding site of p38 MAP kinase. The important residues Tyr35, Thr106, and Met109 are shown in yellow. Also shown in magenta is the position of SB220025.

same side. For compound **44**, forcing these groups into such a position requires 2.6 kcal/mol.

The observations described above together with the activities of **44** compared to **3** and of **45** compared to **40** indicate that the best protein−ligand interactions are obtained when the carbonyl group and the chloro substituent are on the same side. The higher energy penalty for **44** possibly explains why this compound does not have increased activity compared to **3**.

p38 MAP Kinase-Ligand Interaction. Recent works have described the crystal structures of p38α MAP kinase complexed with pyridinyl/pyrimidinyl imidazole inhibitors, e.g. SB220025 and HEP689. These studies have shown that the pyridinyl/pyrimidinyl imidazole inhibitors are ATP-competitive inhibitors.[49−53] Specifically, residue 106 (p38α numbering) has been pinpointed as the most important residue for inhibitor specificity. Thus, potent inhibitors of p38α and p38β MAP kinases but inactive against the isoforms p38γ and p38δ are known. This is explained by the presence of the relatively small threonine in position 106 of p38α and p38β compared to the larger methionine in p38γ and p38δ.[54] The side chain of metheonine blocks access to the hydrophobic region/pocket I in p38γ and p38δ, which in p38α and p38β may be occupied, in the case of SB220025 and HEP689, by the *p*-flourophenyl ring.

We found the benzophenone compounds to be highly potent inhibitors of p38α and p38β isoforms, but they were inactive against the p38γ and p38δ isoforms. This suggests that part of the benzophenone compounds occupy the hydrophobic pocket I and consequently that they bind in the ATP-binding cleft.

As a result of the relatively large and diverse substituents allowed in ring C, we speculated that ring A was most likely to be positioned in the hydrophobic pocket I. To obtain a model of the benzophenone compounds bound to p38α MAP kinase, we docked compound **45** in the ATP-binding cleft using the crystal structure of SB220025 complexed with p38α MAP

kinase[49] as a template (Figure 4). The most important features are the placement of ring A in the hydrophobic pocket and a hydrogen bond between the carbonyl group and the amide proton of Met109 (p38α numbering). Replacement of the carbonyl group, as in compound **70** and **71**, gave significantly lower p38α kinase activity (Table 3). This indicated that the hydrogen bond to the carbonyl group is very important.

The lower activity of compound **60** and others without the secondary amino group (vide supra) suggests that the amino group connecting rings B and C are involved in a hydrogen bond. However, the model does not clearly indicate the potential partner in such a hydrogen bond. The aromatic ring C is essential for activity (data not shown). Unfortunately, the position of ring C in the present model is somewhat arbitrary, due to the lack of consistent SAR data. However, it has been shown that the glycine-rich loop of kinases can undergo significant conformational changes upon ligand binding[49,55] and one might speculate that a conformational change can facilitate favorable interactions with Tyr35 (p38α numbering) which is positioned in the glycine-rich loop.

In Vivo. To evaluate our compounds in vivo, compound **45**, **49**, and **64** were tested in an acute and a chronic murine model of skin inflammation (Tables 5 and 6). Both models are characterized by high levels of IL-1β, which is rapidly synthesized after challenge. Other inflammatory mediators including TNF-α and IL-2 are also up-regulated, but at lower levels compared to the IL-1β level.[56] The compounds were applied topically in acetone, and steroids with clinical relevance were included as positive controls. In the oxazolone model[57] (acute model), inhibition of ear swelling and the myeloperoxidase (MPO) activity (72 h postchallenge) was in the range of 46−54% and 56−57%, respectively (Table 5). In the 12-*O*-tetradecanoylphobol-13-acetate (TPA) model[58] (chronic model) inhibition of ear swelling and the myeloperoxidase (MPO) activity was in the range of 26−37% and 60−79%, respectively (Table 6). Thus, the in vivo antiinflammatory effects of compounds

Table 5. Inhibition of Ear Swelling and MPO Activity of Selected Compounds in Oxazolone-Induced Murine Allergic Contact Dermatitis[a]

	dose (mg/ear)	inhibn of ear swelling (%) postchallenge			inhibn of MPO activity (%)
compd		24 h	48 h	72 h	
HCS-17-but.	0.001	43 ± 3	55 ± 5	55 ± 4	41 ± 6
45	0.5	43 ± 4	46 ± 2	46 ± 5	56 ± 8
49	0.5	35 ± 4	38 ± 6	46 ± 10	56 ± 10
64	0.5	40 ± 7	46 ± 7	54 ± 7	57 ± 5

[a] Values represent the mean inhibition (%) ± SEM of four or five experiments.

Table 6. Inhibition of Ear Swelling, Ear Weight, and MPO Activity of Selected Compounds in TPA-Induced Murine Chronic Irritative Contact Dermatitis[a]

	dose (mg/ear)	inhibition (%)		
compd		ear swelling	ear weight	MPO activity
BMS-17-val.	0.001	41 ± 2	38 ± 2	67 ± 7
45	0.5	37 ± 5	27 ± 6	73 ± 14
49	0.5	27 ± 2	34 ± 2	79 ± 8
64	0.5	26 ± 4	26 ± 2	60 ± 9

[a] Values represent the mean inhibition (%) ± SEM of three to five experiments

45, **49**, and **64** were almost identical in both models and correlated well with the similar potency of the compounds in the inhibition of IL-1β and TNF-α in vitro (Table 1). The included steroids, hydrocortisone-17-butyrate (HCS-17-but.) and betamethasone-17-valerate (BMS-17-val.), gave similar effects in both models compared to our compounds. The chosen dose (0.001 mg/ear) of the steroids was known not to give toxic side effects on spleen and thymus and is clinically relevant in humans.

Conclusion

A novel structural class of aminobenzophenones were optimized as inhibitors of the proinflammatory cytokines TNF-α and IL-1β. The best compounds were potent inhibitors of TNF-α (IC$_{50}$ = 3−8 nM) and IL-1β (IC$_{50}$ = 9−30 nM) in human PBMC's stimulated by LPS. In addition, the compounds **45**, **49**, and **64** were found to be specific inhibitors of the p38α MAP kinase with IC$_{50}$ values of 10, 39, and 4 nM, respectively. A computer model of the interaction of compound **45** with the p38α MAP kinase in the ATP binding pocket was proposed. The model involved a favorable hydrogen bond between the carbonyl group of the benzophenone and the NH of Met-109, positioning ring A in the hydrophobic pocket I of the enzyme. Furthermore, an interaction of ring C and the aromatic ring of Tyr-35 was suggested.

Finally, compound **45**, **49**, and **64** showed antiinflammatory activity in two murine skin models of acute and chronic dermatitis. However, further studies are needed to examine the potential toxicity of these compounds. These and other studies, including the evaluation of our compounds for the treatment of systemic disorders such as RA, are in progress.

Experimental Section

General Procedures. Commercial-grade reagents and solvents were used without further purification except as indicated. THF (Merck Secosolv, max 0.0075% H$_2$O), 1,4-dioxane, dichloromethane (DCM), and toluene were dried by sequential treatment with two portions of 4 Å molecular sieves and then stored in a closed bottle over 4 Å molecular sieves. All reactions were carried out under an inert atmosphere of dry argon. Flash column chromatography was carried out on Merck silica gel 60 (0.040−0.063 mm). Thin-layer chromatography (TLC) analyses were performed on Merck silica gel 60-F$_{254}$ plates and visualized using UV light (254 nm) and/or a solution consisting of ceric ammonium sulfate and hexaammonium heptamolybdate in 10% H$_2$SO$_4$. Melting points were determined in open glass capillaries using a Buchi melting point apparatus and are uncorrected. ^{1}H NMR (300 MHz) and ^{13}C NMR (75 MHz) spectra were recorded on a Bruker ARX-300 spectrometer. Chemical shifts (δ) are reported in parts per million (ppm) relative to TMS as internal standard. Elementary analyses were performed by the analytical department at LEO on home-built combustion equipment. High-resolution electron ionization mass spectra (EIMS) were obtained using a Micromass Autospec spectrometer. No attempt was made to optimize the reported yields.

{**4-[(2-Aminophenyl)amino]phenyl**}**(phenyl)methanone (3).** To a stirred suspension of **29** (10.2 g, 32.0 mmol) in EtOH (300 mL) was added hydrazine hydrate (3.0 mL, 60 mmol) and 10% Pd/C (3.0 g) at room temperature. The reaction mixture was stirred for 24 h, filtered through Celite, and then crystallized by the addition of water (1000 mL). The solid was filtered, washed with water, and dried to yield **3** (8.62 g, 93%) as a solid: mp 115−116 °C; ^{1}H NMR (CDCl$_3$) δ 7.77−7.67 (m, 4H), 7.52 (m, 1H), 7.48−7.38 (m, 2H), 7.14 (m, 1H), 7.08 (dt, 1H), 6.81 (m, 1H), 6.77 (dt, 1H), 6.69 (m, 2H), 5.77 (bs, 1H), 3.80 (bs, 2H); ^{13}C NMR (CDCl$_3$) δ 195.3, 150.0, 142.8, 138.8, 132.8, 131.4, 129.5, 128.1, 127.7, 127.3, 126.7, 125.8, 119.1, 116.3, 113.1.

N-Methoxy-2,N-dimethylbenzamide (6). To a stirred suspension of 2-methylbenzoic acid (1.36 g, 10.0 mmol) in toluene (5.0 mL) were added thionyl chloride (0.8 mL, 11 mmol) and DMF (0.08 mL, 1 mmol). The resulting mixture was refluxed for 2 h and then cooled to ambient temperature and concentrated in vacuo to give the crude acid chloride. The acid chloride was used immediately without any further purification by dissolving it in ethanol-free DCM (20 mL) followed by the addition of *N,O*-dimethylhydroxylamine hydrochloride (1.07 g, 11.0 mmol). The solution was cooled to 0 °C, and pyridine (1.8 mL, 22 mmol) was added. A white solid was rapidly formed (pyridinium hydrochloride). The reaction mixture was stirred at ambient temperature overnight and then poured into a mixture of DCM/ether 1:1 (50 mL). The organic phase was separated, washed with brine (50 mL), dried (Na$_2$SO$_4$), and filtered, and the solvent was evaporated in vacuo to leave a residue, which was purified by flash chromatography eluting with petroleum ether/EtOAc 2:1 to yield **6** (1.68 g, 94%) as an oil: ^{1}H NMR (CDCl$_3$) δ 7.27 (m, 2H), 7.19 (m, 2H), 3.52 (bs, 3H), 3.30 (bs, 3H), 2.33 (s, 3H); ^{13}C NMR (CDCl$_3$) δ 135.3, 134.8, 130.1, 129.2, 126.2, 125.4, 61.0, 32.9, 19.1.

A similar procedure was used to prepare **7**.

(4-Aminophenyl)(2-methylphenyl)methanone (20). *n*-Butyllithium (5.85 mL, 1.68 M in hexane, 9.84 mmol) was added slowly (5 min) to a solution of 4-bromo-*N,N*-bis(trimethylsilyl)aniline (**5**, Aldrich, 3.11 g, 9.84 mmol) in Et$_2$O (15 mL) at 0 °C. After stirring for 1 h, the solution was transferred via a syringe to a precooled (−78 °C) solution of **6** (1.68 g, 9.37 mmol) in THF (10 mL) under stirring, and the resulting reaction mixture was allowed to warm to room temperature overnight. The yellow solution was poured into 1 N HCl (60 mL) and stirred for 15 min. The aqueous phase was neutralized with saturated NaHCO$_3$ and the organic phase separated. The aqueous phase was extracted with DCM/ether (1:1), and the combined extracts were dried over MgSO$_4$ and concentrated in vacuo. The residue was purified by flash chromatography using petroleum ether/EtOAc 2:1 to yield **20** as a yellow sticky solid (1.47 g, 74%): ^{1}H NMR (CDCl$_3$) δ 7.64 (m, 2H), 7.34 (m, 1H), 7.28−7.18 (m, 3H), 6.61 (m, 2H), 4.22 (bs, 2H), 2.28 (s, 3H); ^{13}C NMR (CDCl$_3$) δ 197.1, 151.5, 139.8, 135.8, 132.8, 130.6, 129.4, 127.8, 127.6, 125.1, 113.7, 19.7.

A similar procedure was used to prepare **21**.

(2-Chloro-4-nitrophenyl)(2-methylphenyl)methanone (17). *n*-Butyllithium (13.42 mL, 1.49 M in hexane, 20.0 mmol) was added dropwise (10 min) to a solution of 1-bromo-2-methylbenzene (**10**, 2.41 mL, 20.0 mmol) in THF (20 mL) at −78 °C, and the resulting mixture was stirred for 20 min. A THF solution of dry ZnCl$_2$ (1.0 M, 25 mL) was added with a syringe and the reaction mixture was allowed to warm to room temperature. After 2 h the reaction mixture was cooled to 0 °C, and tetrakis(triphenylphosphine)palladium(0) (1.15 g, 1.00 mmol) was added followed by the addition of 2-chloro-4-nitrobenzoyl chloride (**13**, prepared from 2-chloro-4-nitrobenzoic acid (4.33 g, 21.5 mmol) by treatment with thionyl chloride as described in the synthesis of **6** above) in THF (5 mL). The stirring reaction mixture was allowed to warm to room temperature overnight. The mixture was partitioned between EtOAc (50 mL) and 1 N HCl (100 mL), and the aqueous phase was extracted with EtOAc (50 mL). The combined organic extracts were washed with brine, dried over MgSO$_4$, and concentrated in vacuo. The residue was purified by flash chromatography using petroleum ether/EtOAc 9:1 to yield **17** as a pale yellow solid (4.21 g, 76%): mp 78−80 °C; ^{1}H NMR (CDCl$_3$) δ 8.31 (d, 1H), 8.22 (dd, 1H), 7.58 (d, 1H), 7.47 (dt, 1H), 7.36 (bd, 1H), 7.27 (dd, 1H), 7.22 (bt, 1H), 2.64 (s, 3H); ^{13}C NMR (CDCl$_3$) δ 195.1, 148.9, 145.5, 140.6, 135.0, 133.1, 132.7, 132.4, 131.9, 130.0, 125.9, 125.4, 121.9, 21.5.

A similar procedure was used to prepare **15**, **16**, **18, 19, 22,** and **53**.

(4-Amino-2-chlorophenyl)(2-methylphenyl)methanone (25). A solution of **17** (4.20 g, 15.2 mmol) in absolute

EtOH (30 mL) was added to stannous chloride dihydrate (17.1 g 76.2 mmol) and the resulting mixture was stirred at 70 °C for 2 h. The reaction mixture was cooled to room temperature and poured into ice/water (50 mL), and the pH was made strongly alkaline by the addition of saturated NaOH (100 mL) before being extracted with EtOAc (2 × 100 mL). The organic phases were combined and washed with brine, dried (MgSO$_4$), filtered, and concentrated in vacuo to yield **25** as a light-yellow solid (3.59 g, 96%): mp 94−96 °C; ^{1}H NMR (CDCl$_3$) δ 7.35 (dt, 1H), 7.30 (dd, 1H), 7.28 (d, 1H), 7.24 (bd, 1H), 7.18 (bt, 1H), 6.66 (d, 1H), 6.49 (dd, 1H), 4.19 (bs, 2H), 2.40 (s, 3H); ^{13}C NMR (CDCl$_3$) δ 196.7, 150.5, 139.5, 137.6, 135.1, 133.9, 131.2, 130.7, 129.5, 127.5, 125.3, 116.0, 112.2, 20.3; HRMS (EI) *m/z* 245.0596 [(M$^+$) calcd for C$_{14}$H$_{12}$ClNO 245.0607].

A similar procedure was used to prepare **23**, **24**, **26**, **27**, **40**−**44**, **46**−**49**, **60**, and **70**.

(4-Amino-2-methylphenyl)(2-methylphenyl)methanone (28). A solution of **54** (1.04 g, 2.67 mmol) in THF (10 mL) was added to aqueous 2.0 N HCl (1.0 mL) and then the reaction stirred for 1 h. The reaction mixture was partitioned between aqueous 0.5 N HCl (30 mL) and 2:1 hexane/EtOAc (30 mL). The aqueous layer was separated and made alkaline with 2 N NaOH (20 mL) and then extracted with EtOAc (2 × 30 mL). The organic phases were dried (MgSO$_4$), filtered, and concentrated in vacuo. The residue was purified by flash chromatography using petroleum ether/EtOAc 5:1 to yield **28** as an oil (0.55 g, 91%): ^{1}H NMR (CDCl$_3$) δ 7.32 (dt, 1H), 7.28−7.14 (m, 4H), 6.52 (d, 1H), 6.37 (dd, 1H), 4.03 (bs, 2H), 2.54 (s, 3H), 2.30 (s, 3H); ^{13}C NMR (CDCl$_3$) δ 199.1, 149.9, 142.9, 141.2, 136.3, 135.4, 130.7, 129.6, 128.4, 127.7, 125.2, 117.4, 110.8, 22.0, 19.9.

{2-Chloro-4-[(2-nitrophenyl)amino]phenyl}(2-methylphenyl)methanone (35). A mixture of 1-fluoro-2-nitrobenzene (**50**, 1.65 mL, 15.6 mmol) and **25** (4.00 g, 16.3 mmol) in DMSO (25 mL) was cooled in an ice bath (0 °C). A solution of KO*t*Bu (3.88 g, 34.6 mmol) in DMSO (20 mL) was placed in a dropping funnel and added dropwise over 5 min. The ice bath was removed and the mixture was stirred for 18 h at room temperature. Water (100 mL) was added and after 5 min the reaction mixture was extracted with EtOAc (3 × 100 mL). The combined organic extracts were washed with water and brine, dried (MgSO$_4$), filtered, and concentrated in vacuo. The residue was purified by flash chromatography using petroleum ether/EtOAc 9:1 to yield **35** as a orange solid (3.95 g, 69%): mp 150−152 °C; ^{1}H NMR (CDCl$_3$) δ 9.43 (s, 1H), 8.23 (dd, 1H), 7.55−733 (m, 6H), 7.30 (bd, 1H), 7.22 (m, 2H), 6.95 (m, 1H), 2.53 (s, 3H); ^{13}C NMR (CDCl$_3$) δ 196.4, 142.7, 140.1, 139.0, 137.6, 135.8, 135.1, 134.7, 134.0, 132.2, 131.8, 131.7, 130.6, 126.9, 125.6, 123.0, 119.8, 119.7, 117.1, 20.9; HRMS (EI) *m/z* 366.0771 [(M$^+$) calcd for C$_{20}$H$_{15}$ClN$_2$O$_3$ 366.0771]. Anal. (C$_{20}$H$_{15}$ClN$_2$O$_3$): C, H, N, Cl.

A similar procedure was used to prepare **29**−**34** and **36**−**39**.

{4-[(2-Aminophenyl)amino]-2-chlorophenyl}(2-methylphenyl)methanone (45). This compound was prepared as described in the synthesis of **25** from **35** (14.2 g, 38.8 mmol). The residue was triturated in a mixture of Et$_2$O/petroleum ether (1:1), and the solid was collected by filtration and dried in vacuo to yield **45** as yellow crystals (11.55 g, 89%): mp 113−114 °C; ^{1}H NMR (CDCl$_3$) δ 7.40−7.05 (m, 7H), 6.85−6.74 (m, 2H), 6.69 (d, 1H), 6.55 (dd, 1H), 5.61 (bs, 1H), 3.79 (bs, 2H), 2.42 (s, 3H); ^{13}C NMR (CDCl$_3$) δ 196.5, 149.5, 142.9, 139.3, 137.7, 135.2, 133.7, 131.2, 130.7, 129.5, 128.2, 127.7, 126.9, 125.3, 119.2, 116.4, 115.3, 111.8, 20.4; HRMS (EI) *m/z* 336.1030 [(M$^+$) calcd for C$_{20}$H$_{17}$ClN$_2$O 336.1029]. Anal. (C$_{20}$H$_{17}$ClN$_2$O): C, H, N, Cl.

{2-Chloro-4-[(diphenylmethylene)amino]phenyl}(2-methylphenyl)methanone (54). An oven-dried Schlenk tube was charged with Pd$_2$(dba)$_3$ (15.8 mg, 0.017 mmol) and *rac*-BINAP (32.3 mg, 0.052 mmol) and purged with argon. To the flask were added **53** (1.00 g, 3.46 mmol), benzophenoneimine (0.87 mL, 5.2 mmol), NaO*t*Bu (465 mg, 4.84 mmol), and toluene (9.0 mL), and the mixture was heated to 80 °C and stirred for 48 h. The mixture was cooled to room temperature and filtered

through a pad of silica gel. Silica gel was added to the filtrate, and the solvents were removed in vacuo. The residue was poured onto a column and eluted successively with petroleum ether/DCM 5:1 and petroleum ether/DCM 1:1 to yield **54** as a yellow oil (1.046 g, 78%): ^{1}H NMR (CDCl$_3$) δ 7.85−7.05 (m, 15H), 6.68 (d, 1H), 6.46 (dd, 1H), 2.39 (s, 3H), 2.26 (s, 3H); ^{13}C NMR (CDCl$_3$) δ 200.1, 168.7, 154.3, 140.2, 139.1, 137.1, 135.8, 133.1, 132.4, 131.0, 130.4, 129.4, 128.9, 128.3, 128.0, 125.4, 123.9, 117.4, 21.2, 20.3.

N-(2-{[3-Chloro-4-(2-methylbenzoyl)phenyl]amino}-phenyl)acetamide (56). A mixture of **45** (1.50 g, 4.45 mmol) and acetic anhydride (0.59 mL, 5.9 mmol) in glacial acetic acid (10 mL) was stirred at room temperature for 45 min. Water (15 mL) was added and the mixture was stirred for 10 min before being extracted with EtOAc. The organic layer was separated and concentrated in vacuo. The residue was co-evaporated with cyclohexane (2 × 10 mL) to leave a syrup which crystallized on the addition of petroleum ether/EtOAc 1:1 to yield **56** as a yellow solid (1.42 g, 84%): mp 150−152 °C; ^{1}H NMR (CDCl$_3$) δ 7.71 (s, 1H), 7.60 (dd, 1H), 7.40−7.10 (m, 8 H), 6.81 (d, 1H), 6.64 (dd, 1H), 6.59 (bs, 1H), 2.42 (s, 3H), 2.16 (s, 3H); ^{13}C NMR (CDCl$_3$) δ 196.7, 169.4, 148.7, 139.1, 137.8, 135.1, 133.6, 132.9, 131.7, 131.3, 130.9, 129.6, 128.8, 126.4, 125.8, 125.4, 124.8, 124.0, 116.2, 112.6, 24.1, 20.4; HRMS (EI) *m/z* 378.1146 [(M$^+$) calcd for C$_{22}$H$_{19}$ClN$_2$O$_2$ 378.1135]. Anal. (C$_{22}$H$_{19}$ClN$_2$O$_2$): C, H, N, Cl.

N-(2-{[3-Chloro-4-(2-methylbenzoyl)phenyl]amino}-phenyl)-N-ethylurea (57). To a solution of **45** (6.50 g, 19.3 mmol) in dry pyridine (60 mL) was added ethyl isocyanate (2.06 g, 29.0 mmol) dropwise under stirring. The reaction mixture was stirred for 4 h, diluted with water (60 mL), and cooled in ice−water. Collection of the crystals by filtration and drying in vacuo overnight gave **57** as a yellow solid (7.63 g, 97%): mp 161−162 °C; ^{1}H NMR (DMSO-d_6) δ 8.34 (s, 1H), 8.04 (d, 1H), 7.79 (s, 1H), 7.42 (m, 1H), 7.10−7.34 (m, 6H), 6.96 (m, 1H), 6.67 (m, 2H), 6.57 (m, 1H), 3.07 (m, 2H), 2.29 (s, 3H), 1.02 (t, 3H); HRMS (EI) *m/z* 407.1418 [(M$^+$) calcd for C$_{23}$H$_{22}$ClN$_3$O$_2$ 407.1401]. Anal. (C$_{23}$H$_{22}$ClN$_3$O$_2$): C, H, N, Cl.

Ethyl 2-{[3-Chloro-4-(2-methylbenzoyl)phenyl]amino}-phenylcarbamate (58). A mixture of **45** (337 mg, 1.00 mmol) and K$_2$CO$_3$ (415 mg, 3.0 mmol) in DCM (8.0 mL) was stirred at 0 °C for 10 min. Ethyl chloroformate (217 mg, 2.0 mmol) was added with a syringe and after 1 h the temperature was raised to room temperature. After 28 h the reaction mixture was partitioned between water and DCM. The organic layer was dried (Na$_2$SO$_4$), filtered, and concentrated in vacuo. The residue was purified by chromatography eluting with DCM followed by DCM/EtOAc 50:1 to give a pale yellow syrup which was crystallized from a mixture of petroleum ether/ether to yield **58** as white solid (302 mg, 74%): mp 114−115 °C; ^{1}H NMR (CDCl$_3$) δ 7.82 (d, 1H), 7.40−7.16 (m, 7H), 7.13 (dt, 1H), 6.91 (bs, 1H), 6.75 (d, 1H), 6.60 (dd, 1H), 6.08 (bs, 1H), 4.22 (q, 2H), 2.44 (s, 3H), 1.30 (t, 3H); ^{13}C NMR (CDCl$_3$) δ 196.6, 154.1, 149.1, 139.1, 138.0, 135.0, 133.5, 133.4, 131.3, 130.9, 130.5, 129.7, 129.2, 126.9, 125.0, 124.9, 121.7, 116.1, 112.5, 61.7, 20.5, 14.5; HRMS (EI) *m/z* 408.1238 [(M$^+$) calcd for C$_{23}$H$_{21}$ClN$_2$O$_3$ 408.1241]. Anal. (C$_{23}$H$_{21}$ClN$_2$O$_3$): C, H, N, Cl.

{2-Chloro-4-[methyl(2-nitrophenyl)amino]phenyl}(2-methylphenyl)methanone (59). To a solution of **35** (1.00 g, 2.73 mmol) in THF (10 mL) was added NaH (72 mg, 3.0 mmol) and then, after 15 min, iodomethane (426 mg, 2.94 mmol), and the mixture was stirred for 2 h under reflux. The reaction mixture was partitioned between EtOAc and saturated aqueous NaHCO$_3$ (×3) and then the organic phases were dried (MgSO$_4$), filtered, and concentrated in vacuo. The residue was purified by chromatography eluting with petroleum ether/EtOAc 5:1 to yield **59** as an orange syrup (1.04 g, 100%): ^{1}H NMR (CDCl$_3$) δ 7.99 (dd, 1H), 7.70 (dt, 1H), 7.49 (dt, 1H), 7.42 (dd, 1H), 7.39−7.28 (m, 3H), 7.24 (bd, 1H), 7.18 (bt, 1H), 6.61 (d, 1H), 6.42 (dd, 1H), 3.33 (s, 3H), 2.41 (s, 3H); ^{13}C NMR (CDCl$_3$) δ 196.4, 150.9, 147.3, 139.9, 139.2, 137.8, 135.0, 134.7, 134.6, 133.3, 131.2, 131.2, 130.7, 129.6, 128.1, 126.0, 125.4, 114.8, 111.1, 40.1, 20.4.

{2-Chloro-4-[(4-fluoro-2-methylphenyl)amino]phenyl}-(2-methylphenyl)methanone (64). A Schlenk tube was charged with **25** (737 mg, 3.00 mmol) in 1,4-dioxane (30 mL), 1-bromo-4-fluoro-2-methylbenzene (**61**, 624 mg, 3.30 mmol), Cs_2CO_3 (1.37 g, 4.20 mmol), $Pd_2(dba)_3$ (69 mg, 0.075 mmol), and *rac*-BINAP (140 mg, 0.23 mmol). The tube was capped with a rubber septum, flushed with argon for 5 min, and then stirred at 100 °C for 72 h. The reaction mixture was allowed to cool to room temperature and then poured into a mixture of water and EtOAc. The aqueous phase was extracted with more EtOAc (×2). The combined organic phases were washed with brine, dried ($MgSO_4$), filtered, and concentrated in vacuo. The crude product was purified by chromatography eluting with petroleum ether/ether 4:1 to yield an orange solid (910 mg). Trituration in a mixture of petroleum ether/ether 10:1, filtration, and washing of the solid with petroleum ether/ether 10:1 gave **64** as a yellow solid (733 mg, 69%): mp 151−152 °C; ^{1}H NMR (CDCl$_3$) δ 7.39−7.29 (m, 3H), 7.27−7.14 (m, 3H), 6.99 (dd, 1H), 6.92 (dt, 1H), 6.66 (d, 1H), 6.53 (dd, 1H), 5.65 (s, 1H), 2.42 (s, 3H), 2.23 (s, 3H);^{13}C NMR (CDCl$_3$) δ 196.5, 160.5, 149.6, 139.3, 137.8, 136.3, 135.3, 133.7, 131.2, 130.7, 129.5, 128.2, 127.1, 125.3, 117.8, 115.2, 113.8, 111.6, 20.4, 18.1; HRMS (EI) *m/z* 353.0997 [(M[+]) calcd for $C_{21}H_{17}ClFNO$ 353.0983]. Anal. ($C_{21}H_{17}ClFNO$): C, H, N, Cl.

A similar procedure was used to prepare **62**, **63**, **65**, and **69**.

[2-Chloro-4-(2,5-dimethyl-1*H*-pyrrol-1-yl)phenyl](2-methylphenyl)methanone (66). A 100-mL round-bottom flask was charged with **25** (2.01 g, 8.18 mmol), toluene (70 mL), TsOH·H$_2$O (16 mg, 1 mol %), and acetonylacetone (1.20 g, 10.5 mmol). The solution was warmed to reflux under Dean−Stark conditions for 2.5 h, at which point TLC analysis indicated complete conversion to the pyrrole. The solution was cooled to room temperature, washed with aqueous NaHCO$_3$, dried ($MgSO_4$), filtered, and concentrated in vacuo. The crude product was purified by chromatography eluting with petroleum ether/DCM 2:1 followed by DCM to yield **66** as a white solid (2.49 g, 94%): mp 99−100 °C; ^{1}H NMR (CDCl$_3$) δ 7.53 (d, 1H), 7.44 (dt, 1H), 7.38 (dd, 1H), 7.33 (m, 1H), 7.31 (d, 1H), 7.24 (bt, 1H), 7.20 (dd, 1H), 5.93 (s, 2H), 2.59 (s, 3H), 2.09 (s, 6H); ^{13}C NMR (CDCl$_3$) δ 196.6, 141.7, 139.6, 138.6, 136.7, 132.5, 132.3, 132.0, 131.2, 130.5, 129.9, 128.6, 126.6, 125.7, 106.8, 21.2, 13.1.

1-{3-Chloro-4-[1-(2-methylphenyl)vinyl]phenyl}-2,5-dimethyl-1*H*-pyrrole (67). MeLi (2.82 mL, 1.07 M in THF, 3.02 mmol) was added dropwise (15 min) to a stirred solution of **66** (0.956 g, 29.5 mmol) in THF (30 mL) at −78 °C. The reaction was warmed to 10 °C over a period of 2.5 h and then quenched with saturated aqueous NH$_4$Cl. Extraction with EtOAc (×2), collection of the organic phases, washing with water and brine, and concentration in vacuo gave the crude alcohol, which was used without any further purification. The residue was dissolved in glacial acetic acid (60 mL) and refluxed for 3 h. The cooled reaction mixture was partitioned between water and EtOAc (×2), the organic phases were combined, dried ($MgSO_4$), filtered, and concentrated, and the residue was purified by flash chromatography eluting with petroleum ether/EtOAc 12:1 to yield **67** as a white solid (0.514 g, 54%): mp 139−141 °C; ^{1}H NMR (CDCl$_3$) δ 7.30 (d, 1H), 7.27−7.14 (5H), 7.06 (dd, 1H), 5.89 (bs, 2H), 5.71 (d, 1H), 5.59 (d, 1H), 2.17 (s, 3H), 2.05 (s, 6H); ^{13}C NMR (CDCl$_3$) δ 146.6, 141.1, 140.2, 138.8, 135.7, 132.8, 131.3, 130.6, 129.8, 128.7, 127.7, 126.5, 125.8, 121.4, 106.2, 20.5, 13.0.

3-Chloro-4-[1-(2-methylphenyl)vinyl]phenylamine (68). A thick-walled vial (8 mL) was charged with **67** (233 mg, 0.72 mmol), Et$_3$N (0.44 mL, 3.16 mmol), EtOH (2.5 mL), water (0.86 mL) CHCl$_3$ (0.50 mL), and hydroxylamine hydrochloride (577 mg, 8.30 mmol) and then closed and warmed to 90 °C for 16 h. TLC indicated that there was unreacted starting material left. More Et$_3$N (0.44 mL, 3.16 mmol) and hydroxylamine hydrochloride (550 mg, 7.91 mmol) were added to reaction mixture, and stirring was continued at 100 °C for 8 h. The reaction mixture was allowed to cool to room temperature and then poured into a mixture of ice-cold 1 N HCl and EtOAc.

The aqueous phase was extracted with more EtOAc (×2). The combined organic phases were washed with saturated NaHCO$_3$ and brine and then dried ($MgSO_4$), filtered, and concentrated in vacuo. The residue was purified by chromatography eluting with petroleum ether/DCM 2:1 to yield **68** as an oil (138 mg, 79%): ^{1}H NMR (CDCl$_3$) δ 7.22−7.08 (m, 4H), 6.96 (d, 1H), 6.67 (d, 1H), 6.48 (dd, 1H), 5.55 (d, 1H), 5.39 (d, 1H), 3.68 (bs, 2H), 2.14 (s, 3H); ^{13}C NMR (CDCl$_3$) δ 147.1, 146.4, 142.1, 135.8, 133.1, 131.8, 130.9, 130.3, 129.7, 127.2, 125.5, 119.4, 116.0, 113.3, 20.4.

***N*-[3-Chloro-4-(2-methylbenzyl)phenyl]-*N*-(4-fluoro-2-methylphenyl)amine (71).** A Schlenk tube was charged with CF$_3$COOH (2.50 mL) and cooled to 0 °C. NaBH$_4$ (114 mg, 3.0 mmol) was added in small portions over 5 min and the mixture was stirred for 1 h. A solution of **64** (176 mg, 0.497 mmol) in DCM (1.50 mL) was added over a period of 30 min, the mixture was allowed to warm to room temperature, and stirring was continued for 22 h. More NaBH$_4$ (57 mg, 1.5 mmol) was added to the reaction mixture and stirring was continued for an additional 5 h. The reaction mixture was poured into water, made basic by the addition of NaOH (pellets), and extracted with ether (×2). The combined organic extracts were dried over MgSO$_4$, filtered, and concentrated to a brown solid (206 mg). Flash chromatography using petroleum ether/EtOAc 8:1 gave an almost inseparable mixture of **71** and **72** (approximately 170 mg). A pure sample (7.1 mg) of the undesired compound **72** was obtained. Purification of a small portion (ca 40 mg) of the mixture by preparative gradient HPLC (10 × 250 mm RP column, C-18; mobile phase 0 to 95% CH$_3$CN in water with 0.01% CF$_3$COOH) gave a pure sample of **71** (20 mg) as a hygroscopic solid. **71**: ^{1}H NMR (CDCl$_3$) δ 7.21−7.08 (m, 4H), 7.03−6.82 (m, 3H), 6.81 (d, 1H), 6.72 (d, 1H), 6.55 (dd, 1H), 5.19 (bs, 1H),3.96 (s, 2H), 2.25 (s, 3H), 2.22 (s, 3H).

***N*-[3-Chloro-4-(2-methylbenzyl)phenyl]-*N*-(4-fluoro-2-methylphenyl)-*N*-(2,2,2-trifluoroethyl)amine (72):** ^{1}H NMR (CDCl$_3$) δ 7.20−7.06 (m, 4H), 7.04−6.93 (m, 3H), 6.69 (d, 1H), 6.57 (d, 1H), 6.33 (dd, 1H), 4.13 (m, 2H), 3.94 (s, 2H), 2.23 (s, 3H), 2.08 (s, 3H).

Molecular Modeling. All calculations were performed on a Silicon Graphics O$_2$ R10000 workstation. The conformational and torsional rotational analyses were carried out using the Monte Carlo (Mcrlo) and DRIVE routines of MacroModel 7.0 (Schrödinger Inc.), respectively. The structures were energy-minimized with the Truncated Newton Conjugate Gradient (TNCG) method using the MMFF94s force field, until the default derivative convergence criterion of 0.05 kJ/(mol Å) were met. The solvent was in all MacroModel calculations set to water using the SLVNT command.

Docking of the conformations of compound **45** obtained from a MacroModel conformational search in the ATP-binding pocket of p38α MAP kinase was done using Sybyl 6.7 (Tripos Inc.). We started with the crystal structure of p38α complexed with SB220025[48] (pdb code 1BL7). After removing the water molecules in the PDB file and adding hydrogens, possible identical pharmacophore elements of SB220025 and **45** were superimposed using the *Fit Atoms* facility of Sybyl (Figure 5a). A minor manual adjustment of the position of **45** was done prior to CScore (as implemented in Sybyl 6.7) evaluation of the different conformations. Five conformations had a CScore value of 5, suggesting that these conformations had the best interactions with p38α MAP kinase. These conformations were subjected to further analysis.

As described in the Results and Discussion section, the activity of compound **44** indicates that that the best protein−ligand interactions are obtained when the carbonyl group and the chloro substituent are on the same side. Three of the five conformations of **45** mentioned above have this geometry. Visual inspection of these three conformations revealed that a favorable interaction between ring C and Tyr35 was possible for one conformation. Accordingly, this conformation was chosen to represent the bound conformation of **45**.

Refinement of the p38α−**45** complex was carried out with Sybyl 6.7 using the MMFF94s force field and MMFF94 charges and the following protocol: 500-step Powell energy minimiza-
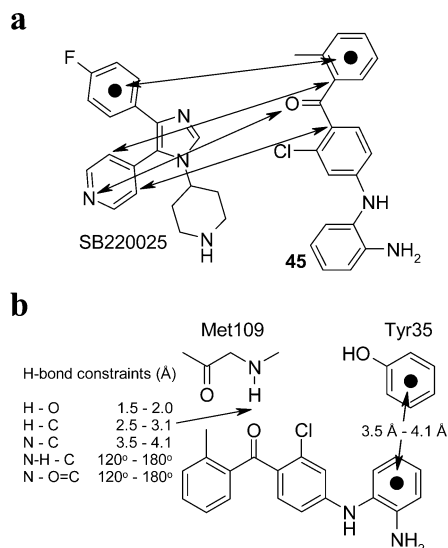
Figure 5. (a) The pharmacophore elements of SB220025 and **45** used in the superposition of these compounds were (1) the centroid of the *p*-flourophenyl ring and the centroid of ring A, (2) the 4-pyridine nitrogen and the carbonyl oxygen, (3) the 2-pyridine carbon and carbon 1 of ring B, and (4) the 6-pyridine carbon and carbon 1 of ring A. (b) The constraints used in the refinement procedure for the H-bond between Met109 and **45** and for the interaction between the Tyr35 ring and ring C.

tion (Initial Optimization parameter set to Simplex) followed by 1 ps molecular dynamics at 300 K and finally 1000-step Powell energy minimization (Initial Optimization parameter set to Simplex). During these calculations constraints were added to maintain a hydrogen bond between the carbonyl group and the amide proton of Met109 and an interaction between ring C and Tyr35 (Figure 5b).

Biological Methods. The in vitro results are expressed as IC_{50} values, where the IC_{50} value is defined as the concentration of compound required to reduce the cytokine levels (or kinase activity) to 50% of control values. All determinations were done in triplicate unless otherwise noted.

Production of cytokines. Human peripheral blood mononuclear cells (PBMC) were isolated from buffy coats. The blood was mixed with saline at a ratio of 1:1, and the PBMC were isolated by the use of Lymphoprep tubes (Nycomed, Norway). The PBMC were suspended in RPMI1640 (no. 42401-018) and supplemented with 2% fetal calf serum (FCS) (IL-1β, TNF-α, IL-6, IL-8, IL-12) or 10% FCS (IL-2, IL-10, IFN-γ) and 2 mM l-glutamine, 100 U penicillin, and 100 mg streptomycin/mL at a concentration of 5×10^5 cells/mL. The cells were preincubated for 30 min with the test compounds in 48- or 96-well tissue culture plates (Life Technologies) and treated as follows:

IL-1β, TNF-α. The cells were stimulated with 1 mg/mL of bacterial endotoxin (LPS) (Sigma L-2880) and incubated (at 37°C with 5% CO_2) for 18 h.

IL-6, IL-8. The cells were stimulated with 1 mg/mL of LPS and incubated for 6 h.

IL-12. The cells were stimulated with 95 ng/mL of IFN-γ for 18 h followed by 1 mg/mL LPS for 24 h.

IL-2, IL-10, IFN-γ. Cells were stimulated with 13, 5, and 3 mg/mL of phytohemagglutinin (no. 3110-57, Becton-Dickinson), respectively, and incubated for 48 h. The levels of cytokines were measured in the culture supernatant by sandwich ELISA [IL-1β, monoclonal antibody no. MAB201 and biotinylated polyclonal antibody no. AB-201-NA (R&D systems, UK); TNF-α, monoclonal antibody no. MAB210 and biotinylated polyclonal antibody no. AB-210-NA (R&D systems, UK); IL-2, monoclonal antibody no. MAB202 and biotinylated polyclonal antibody no. AB-202-NA (R&D systems, UK); IL-6 and IL-8, ELISA kits no. M-1916 and M-1918 (Kem-en-Tec, DK); IL-10, monoclonal antibody no. MAB217 and biotinylated polyclonal antibody no. BAF217; IL-12, monoclonal antibody

against IL-12 p70 and biotinylated polyclonal antibody against p40/p70 (Pharmingen, Becton Dickenson no. 555065 and no. 20512D, respectively); IFN-γ, monoclonal antibody no. MAB285 and biotinylated polyclonal antibody no. BAF285].

Plate Assay for Estimating the Kinase Activity of Compounds for p38 MAP Kinase. The kinase activity of inhibitors of human recombinant p38 MAP kinase was determined using a simple ELISA-based plate assay. The assay was based upon the phosphorylation of the p38 MAP kinase substrate, ATF-2, and was measured using a specific antibody raised against the phosphorylated ATF-2. In brief, Nunc Maxisorb plates were coated with GST-AFT-2 (SantaCruz, sc-4114) (2,5 μg/mL) in 40 mM Tris/HCl pH 7.4, 10 mM magnesium acetate overnight at 4 °C. The plates were blocked with 1% BSA in PBS for 1 h at room temperature. Test compounds were diluted in 25 mM HEPES, pH 7.5, 10 mM magnesium acetate and placed in the coated 96-well microtiter plate. Active p38α (Upstate Ltd. cat. no. 14−251) was diluted in 25 mM HEPES, pH 7.5, 10 mM magnesium acetate and added to the wells in a final concentration of 100 ng/mL. The kinase reaction was allowed to react for 1 h at room temperature. The plate was washed three times with wash buffer (1 × PBS, 0.1% Tween-20) and hereafter incubated with primary antibody, anti-phospho-ATF-2 (F-1) (Santa Cruz, sc-8398), followed by incubation with secondary antibody (rabbit-anti-mouse-HRP, P-0260, DAKO, Denmark). The plates were finally incubated with TMB, and the color reaction was read in an ELISA-reader at A_{460}. The assay was run in duplicate, and the test compounds were diluted from 10^{-10} to 10^{-4}M. The DMSO concentration was 1% final in all concentrations. The data points from three or more individual assays were combined and analyzed by nonlinear regression (GraphPad Prism version 3.00 for Windows, GraphPad software Inc. San Diego, CA). The calculated IC_{50} value is the concentration of the test compound that caused a 50% decrease in the maximal inhibition of p38 MAP kinase activity. In all cases, standard errors were within statistically acceptable limits. A standard compound, SB203580, was included with each set of experiments, and its IC_{50} was 53.3 ± 12.8 nm.

Oxazolone-Induced Murine Allergic Contact Dermatitis. Six female inbreed BALB/cABOM mice per group (weighing 18−21 g; M & B A/S) were sensitized to oxazolone (Sigma Chemical Co.) by application to the clipped abdomen 7 days before challenge with the chemical to the right ear. Twenty microliters of test compound, dissolved in acetone, or vehicle were applied once 30 min after oxazolone challenge. Ear swelling (right ear thickness − left ear thickness) was measured 24, 48, and 72 h postchallenge using a Mitutyo digimatic indicator, and MPO (myeloperoxidase) activity in ear tissue was determined 72 h post challenge. Hydrocortisone-17-butyrate (HCS-17-but.) (Sigma Chemical Co.) was tested as reference compound.[57]

TPA-Induced Murine Chronic Irritative Contact Dermatitis. Skin inflammation in groups of six female inbreed BALB/cABOM mice (weighing 18−21 g; M & B A/S) was induced by phorbol 12-myristate-13-acetate (PMA = TPA from Sigma Chemical Co.) applications to the right ear on days 1, 3, 5, 8, and 10. Twenty microliters to test compound, dissolved in acetone, or vehicle were applied twice daily on days 8, 9, and 10 and once on day 11. Ear swelling, ear weight, and MPO activity in ear tissue were determined 5 h after the last test compound application. Betamethasone-17-valerate (BMS-17-val.) (Sicor) was tested as reference compound.[58]

Determination of Myeloperoxidase Activity. Ear punches were placed in a Teflon shaking flask with a steel ball and frozen in liquid nitrogen. The frozen ear punch was homogenized for 60 s in a Brown Mikrodismembrator U. The obtained powder was transferred to a preweighed Eppendorf tube and reweighed. Then 200 μL of HTAB solution (0.5% in acetate buffer, pH 4.0) per mg of ear powder was added to each tube, and the tubes were shaken on a whirly mixer and incubated for 1 h in a 37° water bath. The tubes were centrifuged at 2500g for 5 min and MPO activity was assayed in the supernatant in quadruplicates as follows: 10

μL of supernatant was mixed in the wells of a microtiter plate with 250 μL of a solution of TMB (385 mg/mL in 0.025% H_2O_2). After 5 min incubation, the absorbance was measured at 655 nm in a micro plate reader (Bio-Rad, model 450). MPO activity was expressed in arbitrary units, one unit being defined as the activity yielding 100 mE in 5 min under the above-described conditions.

Supporting Information Available: The complete experimental procedures with spectroscopical and analytical data for the compounds **7**, **15**, **16**, **18**, **19**, **21**−**24**, **26**, **27**, **29**−**34**, **36**−**39**, **40**−**44**, **46**−**49**, **53**, **60**, **62**, **63**, **65**, **69**, **70**, and **71**. This material is available free of charge via the Internet at http://pubs.acs.org.

References

(1) Dinarello, C. A. Inflammatory cytokines: Interleukin-1 and tumor necrosis factor as effector molecules in autoimmune diseases. *Curr. Opin. Imm.* **1991**, *3*, 941−948.

(2) Arend, W. P.; Dayer, J.-M. Cytokines and cytokine inhibitors or antagonists in rheumatoid arthritis. *Arthitis Rheum.* **1990**, *33*, 305−15.

(3) Dayer, J. M.; Demczuk, S. Cytokines and other mediators in rheumatoid arthritis. *Springer Semin. Immunopathol.* **1984**, *7*, 387−413.

(4) Barnes, P. J.; Chung, K. F.; Page, C. P. Inflammatory mediators of asthma: An update. *Pharmacol. Rev.* **1998**, *50*, 515−596.

(5) Loyau, G.; Punol, J. P. The role of cytokines in the development of osteoarthritis. *Scand. J. Rheumaol Suppl.* **1990**, *81*, 8−12.

(6) Kirkham, B. Interluekin-1, Immune activation pathways and different mechanisms in osteoarthitis and rheumatoid arthritis. *Ann. Rheum. Dis.* **1991**, *50*, 395−400.

(7) Nickoloff, B. J. The cytokine network in psoriasis. *Arch. Dermatol.* **1991**, *135*, 1104.

(8) Saklavala, J.; Davis, W.; Guesdon, F. Interleukin 1 (IL-1) and tumor necrosis factor (TNF) signal transduction. *Philos. Trans. R. Soc. London B.* **1996**, *351*, 151−157.

(9) Sacca, R.; Cuff, C. A.; Ruddle, N. H. Mediators of inflammation. *Curr. Opin. Imm.* **1997**, *9*, 851−857.

(10) Lewis, A. J.; Manning, A. M. New targets for antiinflammatory drugs. *Curr. Opin. Chem. Biol.* **1999**, *3*, 489−494.

(11) Sekut, L.; Connolly, K. M. Pathophysiology and regulation of TNFa in inflammation. *DN&P* **1996**, *9*, 261−269.

(12) Elliott, M. J.; Maini, R. N. New directions for biological therapy in rheumatoid arthritis. *Int. Arch. Allergy. Immunol.* **1994**, *104*, 112−115.

(13) Moreland, L. W.; Heck, L. W., Jr.; Koopam, W. J. Biological therapy in rheumatoid arthritis: Concepts and progress. *Arthritis Rheum.* **1997**, *40*, 397−409.

(14) Lee, J. C.; Kumar, S.; Griswold, D. E.; Underwood, D. C.; Votta, B. J.; Adams, J. L. Inhibition of p38 MAP kinase as a therapeutic strategy. *Immunopharmacol.* **2000**, *47*, 185−201.

(15) Lee, J. C.; Laydon, J. T.; McDonnell, P. C.; Gallagher, T. F.; Kumar, S.; Green, D.; McNulty, D.; Blumenthal, M. J.; Heys, J. R.; Landvatter, S. W.; Strickler, J. E.; McLaughlin, M. M.; Siemens, I. R.; Fisher, S. M.; Livi, G. P.; White, J. R.; Adams, J.; Young, P. R. A protein kinase involved in the regulation of inflammatory cytokine biosynthesis. *Nature* **1994**, *372*, 739−746.

(16) Young, P. R.; McDonnell, P.; Dunnington, D.; Hand, A.; Laydon, J.; Lee, J. C. Pyridinyl imidazoles inhibit IL-1 and TNF production at the protein level. *Agents Actions* **1993**, *39*, C67−C69.

(17) Han, J.; Lee, J. D.; Bibbs, L.; Ulevitch; R. J. A MAP kinase targeted by endotoxin and hyperosmolarity in mammalian cells. *Science* **1994**, *265*, 808−811.

(18) Lee, J. C.; Young, P. R. Role of CSBP/p38/RK stress response kinase in LPS and cytokine signaling mechanisms. *J. Leukoc. Biol.* **1996**, *59*, 152−157.

(19) Raingeaud, J.; Whitmarsh, A. J.; Barrett, T.; Derijard, B.; Davis, R. J. MKK3- and MKK6-regulated gene expression is mediated by the p38 mitogen-activated protein kinase signal transduction pathway. *Mol. Cell. Biol.* **1996**, *16*, 1247−1255.

(20) Beyaert, R.; Cuenda, A.; Vanden-Berghe, W.; Plaisance, S.; Lee, J. C.; Haegeman, G.; Cohen, P.; Fiers, W. The p38/RK mitogen-activated protein kinase pathway regulates interleukin-6 synthesis in response to tumor necrosis factor. *EMBO J.* **1996**, *15*, 1914−1923.

(21) Ono, K.; Han, J. The p38 signal transduction pathway: Activation and function. *Cellular Signaling* **2000**, *12*, 1−13.

(22) Herlaar, E.; Brown, Z. p38 MAPK signaling cascades in inflammatory disease. *Mol. Med. Today* **1999**, *5*, 439−447.

(23) Gallagher, T. F.; Seibel, G. L.; Kassis, S.; Laydon, J. T.; Blumenthal, M. J.; Lee, J. C.; Lee, D.; Boehm, J. C.; Fier Thompson, S. M.; Abt, J. W.; Soreson, M. E.; Smietana, J. M.; Hall, R. F.; Garigipati, R. S.; Bender, P. E.; Erhard, K. F.; Krog, A. J.; Hofmann, G. A.; Sheldrake, P. L.; McDonnell, P. C.; Kumar, S.; Young, P. R.; Adams, J. L. Regulation of stress-induced cytokine production by pyridinylimidazoles; inhibition of CSBP kinase. *Bioorg. Med. Chem.* **1997**, *5*, 49−64.

(24) Badger, A. M.; Bradbeer, J. N.; votta, B.; Lee, J. C.; Adams, J. L.; Griswold, D. E. Pharmacological profile of SB203580, a selective inhibitor of cytokine suppressive binding protein(p38 kinase, in animal models of arthritis, bone resorption, endotoxin shock and immune function. *J. Pharm Exp. Ther.* **1996**, *279*, 1453−1461.

(25) Jackson, J. R.; Bolognese, B.; Hillegass, L.; Kassis, S.; Adams, J.; Griswold, D. E.; Winkler, J. D. Pharmacological effects of SB220025, a selective inhibitor of p38 mitogen-activated protein kinase, in angiogenesis and chronic inflammatory disease models. *J. Pharmacol. Exp. Ther.* **1998**, *284*, 687−692.

(26) Hanson, G. H. Inhibitors of p38 kinase. *Exp. Opin. Ther. Patents* **1997**, *7*, 729−733.

(27) Boehm, J. C.; Adams, J. L. New inhibitors of p38 kinase. *Exp. Opin. Ther. Patents* **2000**, *10*, 25−37.

(28) Salituro F. G.; Germann, U. A.; Wilson, K. P.; Bemis, G. W.; Fox, T.; Su, M. S−S. Inhibitors of p38 MAP kinase: Therapeutic intervention in cytokine-mediated diseases. *Curr. Med. Chem.* **1999**, *6*, 807−823.

(29) Dumas, J.; Sibley, R.; Riedl, B.; Monahan, M. K.; Lee, W.; Lowinger, T. B.; Redman, A. M.; Johnson, J. S.; Kingery-wood, J.; Scott, W. J.; Smith, R. A.; Bobko, M.; Schoenleber, R.; Ranges, G. E.; Housley, T. J.; Bhargava, A.; Wilhelm, S. M.; Shrikhande, A. Discovery of a new class of p38 kinase inhibitors. *Bioorg. Med. Chem. Lett.* **2000**, *10*, 2047−2050.

(30) Redman, A. M.; Johnson, J. S.; Dally, R.; Swartz, S.; Wild, H.; Paulsen, H.; Caringal, Y.; Gunn, D.; Renick, J.; Osterhout, M.; Kingery-Wood, J.; Smith, R. A.; Lee, W.; Dumas, J.; Wilhelm, S. M.; Housley, T. J.; Bhargava, A.; Ranges, G. E.; Shrikhande, A.; Young, D.; Bombara, M.; Scott, W. J. p38 kinase inhibitors for the treatment of arthritis and osteoporosis: Thienyl, furyl and pyrrolyl ureas. *Bioorg. Med. Chem. Lett.* **2001**, *11*, 9−12.

(31) Substituted pyrazoles as p38 kinase inhibitors. *Exp. Opin. Ther. Patents* **1999**, *9*, 975−979.

(32) p38 inhibitors based on the pyridylurea and pyridylacetoamide templates. *Exp. Opin. Ther. Patents* **2000**, *10*, 1151−1154.

(33) Ferraccioli, G. F. VX-745 Vertex Pharmacuetical. *Curr. Opin. Anti-inflam. Immunomod. Invest. Drugs* **2000**, *2*, 74−77.

(34) Pargellis, C.; Regan, J. Inhibitors if p38 mitogen-activated protein kinase for the treatment of rheumatoid arthritis. *Curr. Opin. Invest. Drugs* **2003**, *4*, 566−571

(35) Pratt, J. R.; Massey, W. D.; Pinkerton, F. H.; Thames, S. F. Organosilicon compounds. XX. Synthesis of aromatic diamines via trimethylsilyl-protecting aniline intermediates. *J. Org. Chem.* **1975**, *40*, 1090−1094.

(36) Weinreb, M.; Nahm, S. N-Methoxy-*N*-methylamides as effective acylating agents. *Tetrahedron Lett.* **1981**, *22*, 3815−3818.

(37) Negishi, E.-i.; Bagheri, V.; Chatterjee, S.; Luo, F.-T.; Miller, J. A.; Stoll, A. T. Palladium-catalyzed acylation of organozincs and other organometallics as a convenient route to ketones. *Tetrahedron Lett.* **1983**, *24*, 5181−5184.

(38) Evans, P. A.; Nelson, J. D.; Stanley, A. L. Directed lithiation/transmetalation approach to palladium-catalyzed cross-coupling acylation reactions. *J. Org. Chem.* **1995**, *60*, 2298−2301.

(39) Bumagin, N. A.; Ponomaryov, A. B. Palladium- and nickel-catalyzed aryl- and acyl-demetalation of organometallic compounds. *J. Organomet. Chem.* **1985**, *291*, 129−132.

(40) Bellamy, F. D.; Ou, K. Selective reduction of aromatic nitro compounds with stannous chloride in non acidic and non aqueous medium. *Tetrahedron Lett.* **1984**, *25*, 839−842.

(41) Buchwald, S. L.; Wolfe, J. P.; Åhman, J.; Sadighi, J. P.; Singer, R. A. An ammonia equivalent for the palladium-catalyzed amination of aryl halides and triflates. *Tetrahedron Lett.* **1997**, *38*, 6367−6370.

(42) Gorvin, J. H. The synthesis of di- and tri-arylamines through halogen displacement by base-activated arylamines: Comparison with the Ullmann condensation. *J. Chem. Soc., Perkin Trans. 1* **1988**, 1331−1335.

(43) Buchwald, S. L.; Wolfe, J. P. Improved functional group compatibility in the palladium-catalyzed amination of aryl bromides. *Tetrahedron Lett.* **1997**, *38*, 6359−6362.

(44) Ragan, J. A.; Makowski, T. W.; Castaldi, M. J.; Hill, P. D. 2,5-Dimethylpyrrole protection facilitates cupper(I)-mediated methoxylations of aryl iodides in the presence of anilines. *Synthesis* **1998**, *11*, 1599−1603.

(45) Gribble, G. W.; Kelly, W. J.; Sanford, E. Reactions of sodium borohydride in acidic media; VII. Reduction of diaryl ketones in trifluoroacetic acid. *Synthesis* **1978**, *10*, 763−765.

(46) Jiang, Y.; Gram, H.; Zhao, M.; Gu, J.; Feng, L.; Padova, F. D.; Ulevitch, R. J.; Han, J. Characterization of the structure and function of the fourth member of the p38 group mitogen-activated protein kinase, p38δ. *J. Biol. Chem.* **1997**, *272*, 30122−30128.

(47) Fjording, M. S. Unpublished results

(48) Menéndez, M.; Laynez, J.; Medrano, F. J.; Andreu, J. M. A Thermodynamic Study of the Interaction of Tubulin with Colchicine Site Ligands. *J. Biol. Chem.* **1989**, *264*, 16367−16371.

(49) Wang, Z.; Canagarajah, B. J.; Boehm, J. C.; Kassisà, S.; Cobb, M. H.; Young, P. R.; Abdel-Meguid, S.; Adams, J. L.; Goldsmith, E. J. Structural Basis of Inhibitor Selectivity in MAP Kinases. *Structure* **1998**, *6*, 117−1128

(50) Wilson, K. P.; McCaffrey, P. G.; Hsiao, K.; Pazhanisamy, S.; Galullo, V.; Bemis, G. W.; Fitzgibbon, M. J.; Caron, P. R.; Murcko, M. A.; Su, M. S. S. The Structural Basis for the Specificity of Pyridinylimidazole Inhibitors of p38 MAP Kinase. *Chem. Biol.* **1997**, *4*, 423−431.

(51) Lisnock, JM.; Tebben, A.; Frantz, B.; O'Neill, E. A.; Croft, G.; O'Keefe, S. J.; Li, B.; Hacker, C.; de Laszlo, S.; Smith, A.; Libby, B.; Liverton, N.; Hermes, J.; LoGrasso, P. Molecular Basis for p38 Protein Kinase Inhibitor Specificity. *Biochemistry* **1998**, *37*, 16573−16581.

(52) Liu, Y.; Bishop, A.; Witucki, L.; Kraybill, B.; Shimizu, E.; Tsien, J.; Ubersax, J.; Blethrow, J.; Morgan, D. O.; Shokat, K. M. Structural Basis for Selective Inhibition of Src Family Kinases by PP1. *Chem. Biol.* **1999**, *6*, 671−678.

(53) Schindler, T.; Sicheri, F.; Pico, A.; Gazit, A.; Levitzki, A.; Kuriyan, J. Crystal Structure of Hck in Complex with a Src Family-Selective Tyrosine Kinase Inhibitor. *Mol. Cell.* **1999**, *3*, 639−648.

(54) Gum, R. J.; McLaughlin, M. M.; Kumar, S.; Wang, Z.; Bower, M. J.; Lee, J. C.; Adams, J. L.; Livi, G. P.; Goldsmith, E. J.; Young, P. R. Acquisition of Sensitivity of Stress-activated Protein Kinases to the p38 Inhibitor, SB 203580, by Alteration of One or More Amino Acids within the ATP Binding Pocket. *J. Biol. Chem.* **1998**, *273*, 15605−15610.

(55) Toledo, L. M.; Lydon, N. B.; Elbaum, D. The Structure-Based Design of ATP-site Directed Protein Kinase Inhibitors. *Curr. Med. Chem.* **1999**, *6*, 775−805.

(56) Skak-Nielsen, T.; Tranholm, M.; Hansen, J. R. Unpublished results.

(57) Grabbe, S.; Schwarts, T. Immunoregulatory mechanisms involved in elicitation of allergic contact hypersensitivity. *Rev. Immunol. Today* **1998**, *19*, 37−44.

(58) Alford, J. G.; Stanley, P. L.; Todderud, G.; Tramposch, K. M. Temporal infiltration of leukocyte subsets into mice skin inflamed with phorbol ester. *Agents Action* **1992**, *37*, 260−267.